Titania Electrodes for Generation of Cold Atmospheric Plasma

Plasma technology has been successful in various industries to manufacture or refine products for decades. In recent years cold plasma devices that work near room temperature concur new applications in the medical field, for hygiene purposes but also in the industry and household.

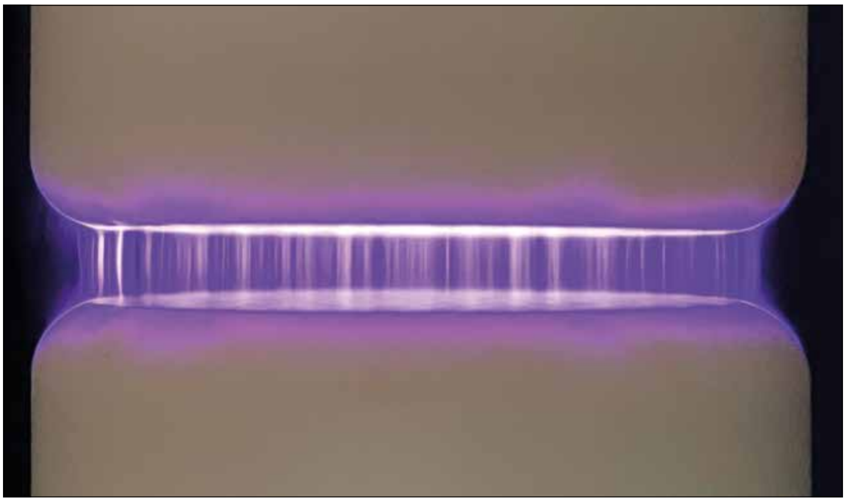

Fig. 1
Cold atmospheric plasma created by dielectric barrier discharge

1 Introduction
Plasma is the fourth state of matter – additionally to solid, liquid, and gaseous state – and describes a (partially) ionized gas. While totally ionized plasma, as in the sun, is several million degrees hot, in cold plasma only the electrons have some 10 000 °C. The gas molecules themselves stay near room temperature.
Therefore, cold plasma can be used safely for temperature sensitive objects such as human tissue or thermoplastics like ABS (Acrylonitrile-Butadiene-Styrene-Copolymer). Cold atmospheric pressure plasma technology is significantly more cost-efficient and versatile than low pressure plasma technology as no vacuum needs to be applied. This allows the devices to be small and mobile in use. Handheld devices are used in the trade, for example to cure silicone or adhesion agents in silicone joints.
Perhaps, the greatest potential of cold atmospheric plasma (Fig. 1) lies in the field of germ control. When in contact with plasma, the electrons, ions, and radicals bombard the cell walls of bacteria, the virus envelopes or other molecules and destroy them by physical interaction [1, 2]. This allows for food sterilization or disinfection in hospitals. In the field of plasma medicine, cold atmospheric pressure plasmas are used to treat human skin. Cold plasmas improve the healing of wounds or diseases on the skin. For example, it stimulates microcirculation in human skin or kills bacteria or viruses that inhibit healing, by acidifying the skin and the reactive species produced by the plasma [3, 4]. Plasma permeabilization of the skin can, among other things, break down the skin's barrier function so that drugs can penetrate and work better [5, 6]. High throughput air cleaning can be applied in commercial kitchens, hospitals, offices, waiting rooms or in animal stables to reduce odour nuisance, pollutants, and germ contamination [7, 8]. Recently, a battery-operated plasma comb was developed that reliably kills lice and nits without the use of chemical agents. The electrons and ions of the plasma create a hostile situation for the lice and are at moderate temperature that the hair and scalp remain undamaged [9,10]. In the electronics and semiconductor industries, plasma treatment is performed to modify surfaces. Plasma coating can be used to make wood more weather-resistant by depositing polymers or metal oxides, or to deposit metals onto temperature-labile surfaces [11, 12].
One way to generate a cold plasma is a Dielectric Barrier Discharge (DBD) (Fig. 2). For this purpose, at least one electrical

Keywords
titania, ceramic injection moulding, dielectric barrier discharge DBD, cold atmospheric plasma, electrode

Anne Mannschatz, Katrin Schönfeld, Axel Müller-Köhn, Hans-Peter Martin
Fraunhofer Institute for Ceramic Technologies and Systems – IKTS
01277 Dresden, Germany

Jannik Schulz, Wolfgang Viöl
HAWK – University of Applied Sciences and Art, Faculty for Engineering and Health
37085 Göttingen, Germany

Corresponding author: A. Mannschatz
E-mail: anne.mannschatz@ikts.fraunhofer.de

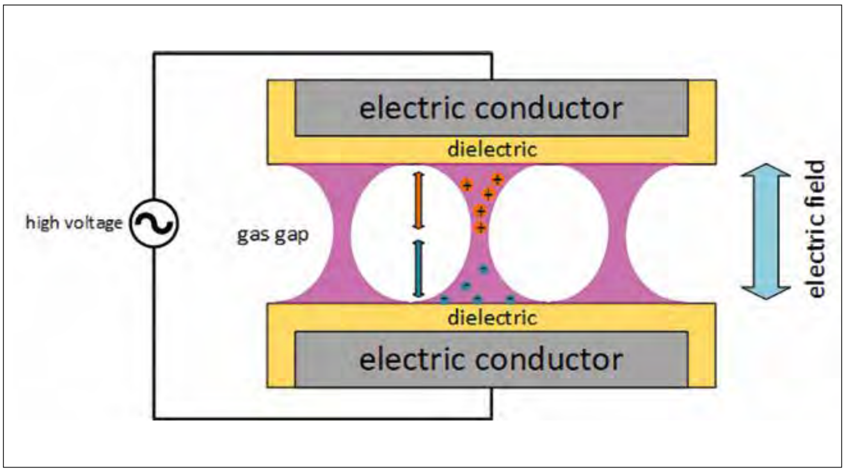

Fig. 2
Typical build of dielectric barrier discharge

conductor at high-voltage potential is surrounded by an insulator (dielectric). The electrical conductor and insulator together form an electrode, which can be positioned either opposite another electrode, conductive material, or surface (opposite pole). With the help of high voltage, an electric field is generated in the discharge space between the electrode and the opposite pole, which is flooded by a gas. If the electric field strength is high enough, plasma ignition occurs. Electrons and ions separate, the gas becomes electrically conductive and reactive species are formed.

Typical working gases are air, argon, hydrogen, or helium. The dielectric barrier prevents the charge carriers from flowing away at the interfaces of the electrodes, so that the current flow of a single discharge comes to a standstill. Due to the dielectric barrier, the discharge is thus slowed down. This allows mainly the light electrons to absorb energy, so that they usually reach several ten thousand Kelvin. The slow ions, on the other hand, remain cold. To maintain the plasma in the gas gap, the voltage direction must be permanently reversed (AC-voltage) so that the charge carriers can continue to flow in the opposite direction.

First atmospheric plasma devices are already available. Currently used plasma electrodes are made of plastics, silicone, ceramics, glass, and metal. However, they do not always fully meet the customer expectations because they wear out relatively quickly what leads to instabilities. Ceramics have a higher stability compared with polymeric materials. Combinations of insulating and conductive ceramics can extend the lifetime of the electrodes.

2 Titania for plasma electrodes

Titanium-oxygen compounds occur in a variety of modifications. Due to the strong interaction between titanium and oxygen and the high oxygen mobility, it is possible to create a variety of different lattice structures. These compounds range from TiO_2, which has a rutile structure, to rutile-like structures of the so called Magnéli phases, strongly reduced oxides such as Ti_3O_5 and Ti_2O_3 with corundum structures and finally TiO and Ti_2O, where oxygen atoms are incorporated into the hexagonal titanium lattice. Due to this oxygen variability, it is possible to shift the intrinsically non-conductive TiO_2 into a conductive suboxide (Fig. 3). The conductivity is caused by free electrons derived from lattice vacancies. Additionally, oxygen ions can contribute by their movement, but they need thermal activation. The dependence of the electrical conductivity on the oxygen content in the Ti–O lattice was investigated by [13, 14].

The nonstoichiometric suboxides of titanium, the so-called Magnéli phases Ti_nO_{2n-1} ($4 \leq n \leq 10$) are of particular importance. These crystallize in the triclinic crystal system, with the lattice spacing differing between the individual Magnéli Phases in the c-direction. This triclinic lattice structure ensures free electrons, which induce the electrical conductivity

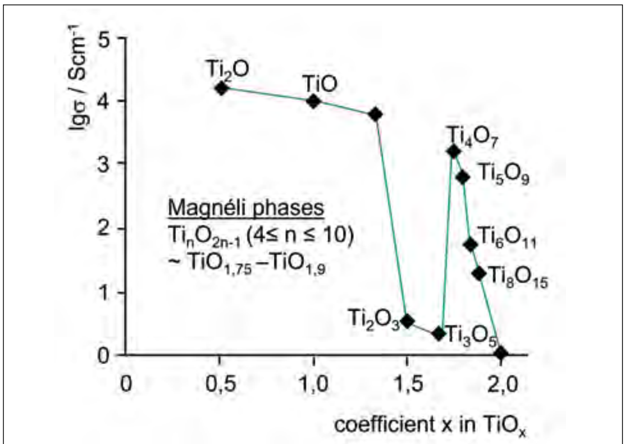

Fig. 3
Change of the electrical conductivity with the oxygen content x in the TiO_x, modified [13]

Tab. 1
Properties of TiO_2 and TiO_x component of the ceramic plasma electrode

Property	TiO_2	TiO_x
Density [g/cm³]	4,12	4,11
Theoretical density [%]	97	96
Young's modulus [GPa]	245 ± 4,6	199 ± 0,5
4PB strength [MPa]	112 ± 26	182 ± 15
Thermal conductivity [W/(m·K)]	6,1	2,2
Electrical resistivity [Ωcm]	$1{,}41 \cdot 10^{12}$	$2 \cdot 10^{-3}$
Breakdown strength [kV/mm]	29,6	
Permittivity (50 Hz)	100	

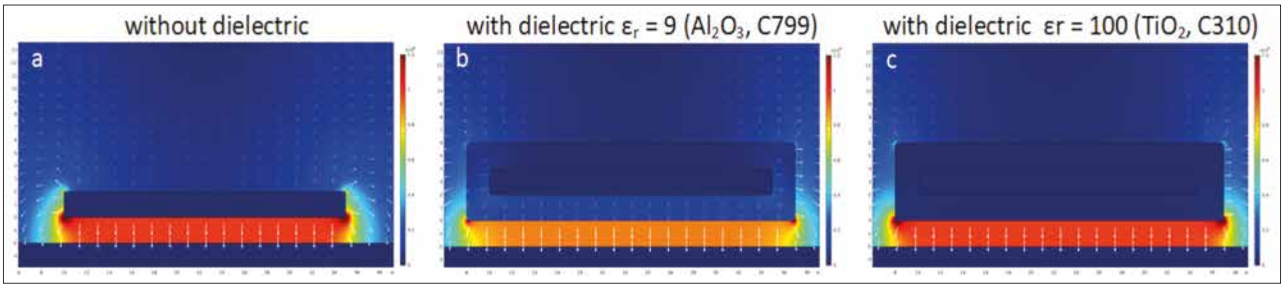

Fig. 4 a–c
Electric field from 0 (blue) to 1,2 e4 (red) V/m by 20 kV power supply: a) without a dielectric, b) with a dielectric with ε_r = 9 like alumina, and c) with a dielectric with ε_r = 100 like titania [14]

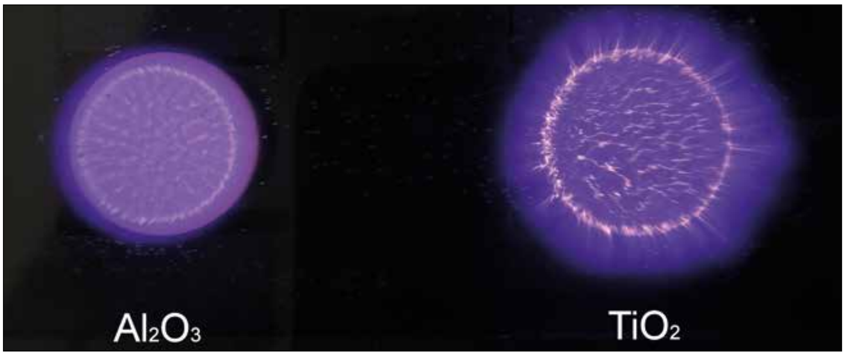

Fig. 5
Two plasma electrodes operated with the same voltage with alumina and titania dielectrics

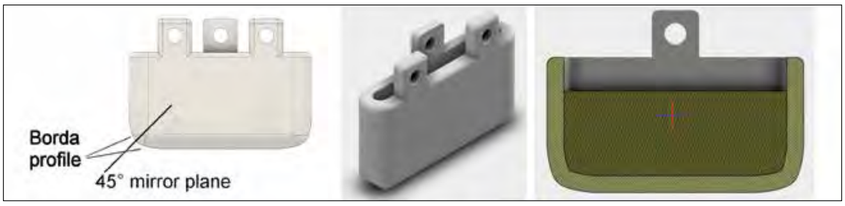

Fig. 6
Design of the plasma electrode with mirrored Borda profile left and right

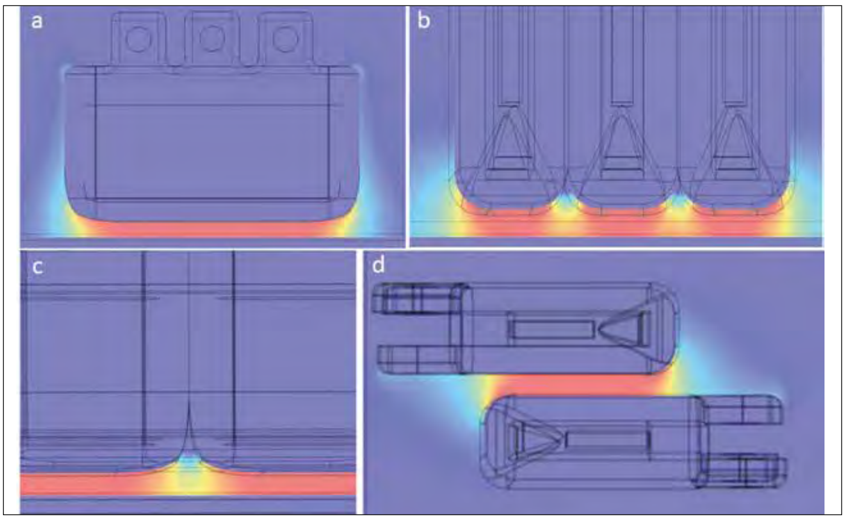

Fig. 7 a–d
Different types of electrode arrangement: a) one electrode against a substrate, b) multiple electrodes stacked on the large flat surface, c) multiple electrodes stacked on the round surface, and d) one electrode against another electrode on the large flat surface

of these materials. Thus, different phases and consequently different electrical conductivity can be created by controlling the oxygen content in titanium oxide. This is accomplished by choosing suited sintering atmospheres and temperatures for oxidizing or reducing. According to the atmosphere in the furnace, oxygen atoms move into or out of the lattice. Those changes of the crystalline system are reversible, but since they are associated with volume changes cracks might form.

The authors used a TiO_x-powder with an oxygen content of x = 1,6 for the conductor which has as main crystalline phase Ti_4O_7. After sintering under argon atmosphere, the Ti_4O_7 remained with $Ti_{10}O_{18}$ as minor phase. The TiO_x composite resulted in a low resistivity of 2·10^{-3} cm which is suitable for the desired application (Tab. 1).

The insulator, the stoichiometric TiO_2 component, was sintered in air reaching a density of 97 %. It acts as dielectric barrier and has two counteracting main tasks. On the one hand, it shall separate the two electrodes and prevent a breakthrough between the two electrodes. The authors achieved a dielectric strength of 29,6 kV/mm which determines the minimum wall thickness of the insulator component. On the other hand, the insulator shall not attenuate the electrical field too much to achieve a high plasma response. Simulations show the effect of different dielectric barriers in the gap of two electrode surfaces (Fig. 4). The strongest electric field forms without a dielectric material, but then no DBD takes place, and the plasma is hot. If alumina (ε_r = 9), which is a typically used material in DBD electrodes, is applied the electric field is attenuated by about 10 %. This means that higher voltages need to be applied to ignite and

Fig. 8
Mould for producing insulator and conductor component

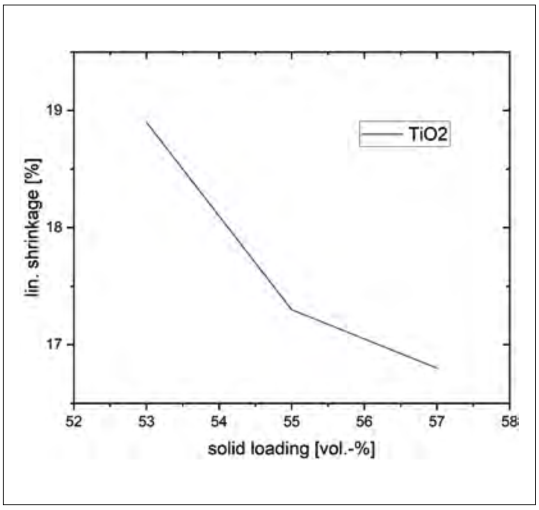

Fig. 9
Solid loading of the feedstock and resulting shrinkage

Fig. 10
Sintered TiO_2-insulator and TiO_x-conductor, ready to be joined by an adhesive

maintain the plasma. Titania has an ε_r of 100. This considerably higher permittivity results in higher electrical fields, which is attenuated only by about 1 % and the ignition voltage in the gas gap (ε_r = 1) is reached earlier. The lower reduction of the electric field strength in the dielectric is due to the increased electric flux, which depends on the permittivity ($\vec{D} = \varepsilon_0 \varepsilon_r \vec{E}$) or the associated higher capacitive coupling. This means that operating voltages can be reduced by 9 % for the same electric field in the gap.

Fig. 5 shows the plasma of an alumina and titania electrode of the same size which are connected in parallel against the same counter electrode. It can be seen that the plasma is more pronounced, it covers a larger area and is brighter for the titania electrode with the higher permittivity. A transparent counter electrode has been used.

3 Manufacturing of electrodes

The electrode is designed as example for various application scenarios. It has two large flat surfaces (front and back), two rounded surfaces (left and right), one flat surfaces (bottom) and three mounting lugs (top). The electrode (Fig. 6) can be used alone against a substrate, against another electrode or as stack with multiple electrodes (Fig. 7). This functional design allows to treat different materials like large planes or high gas volumes. The electrical field should be homogeneous in the gap since field peaks pose the risk of breakdowns and filamentation of the plasma. To prevent an increase of the electric field at corners and edges, all corners and edges are rounded.

Along the short edge runs a Border profile, which is mirrored at the 45° plane, to eliminate electric field increase to the bottom, left and right. Due to the dielectric strength of the TiO_2 the thickness of the insulator is 2,5 mm and the TiO_x (conductor) has a thickness of 3 mm.

Due to the complex shape of the insulator, powder injection moulding was chosen for manufacturing the parts [16]. The mould contains two cavities (Fig. 8) one for the conductor and one for the insulator. Feedstocks for TiO_2 and TiO_x were developed using a PE-wax-based binder system which is soluble in isopropanol by 54 %. In this way pores are opened and thermal debinding can be carried out faster without producing cracks. The viscosity of the binder system allows for adjusting the solid loading in a wider range (Fig. 9). The higher the binder content, the lower the packing density is. Since the binder takes up volume the particle spacing and hence the shrinkage is increased. With a constant sintered density for all cases, shrinkage was 16,8 % and 18,9 % for solids loadings of 57 vol.-% and 53 vol.-%, respectively. In choosing the low solid loading for the inner TiO_x component and the high solid loading for the outer component, a gap was produced which was big enough to fit the two parts into each other (Fig. 10).

Additionally, thickness of the conductor was further reduced by green machining. After sintering, insulator and conductor were joined by a conductive adhesive con-

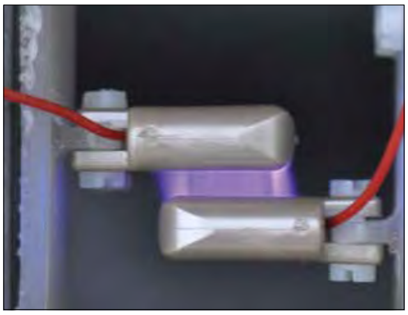

Fig. 11
Electrode build for long time operation

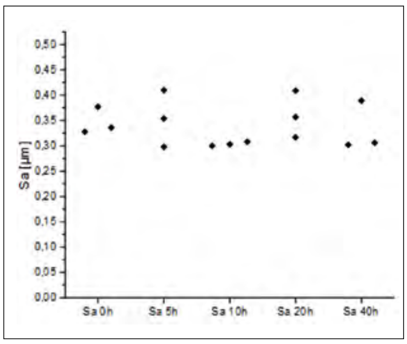

Fig. 12
Surface roughness at 0, 5, 10, 20 and 40 h operating time, respectively

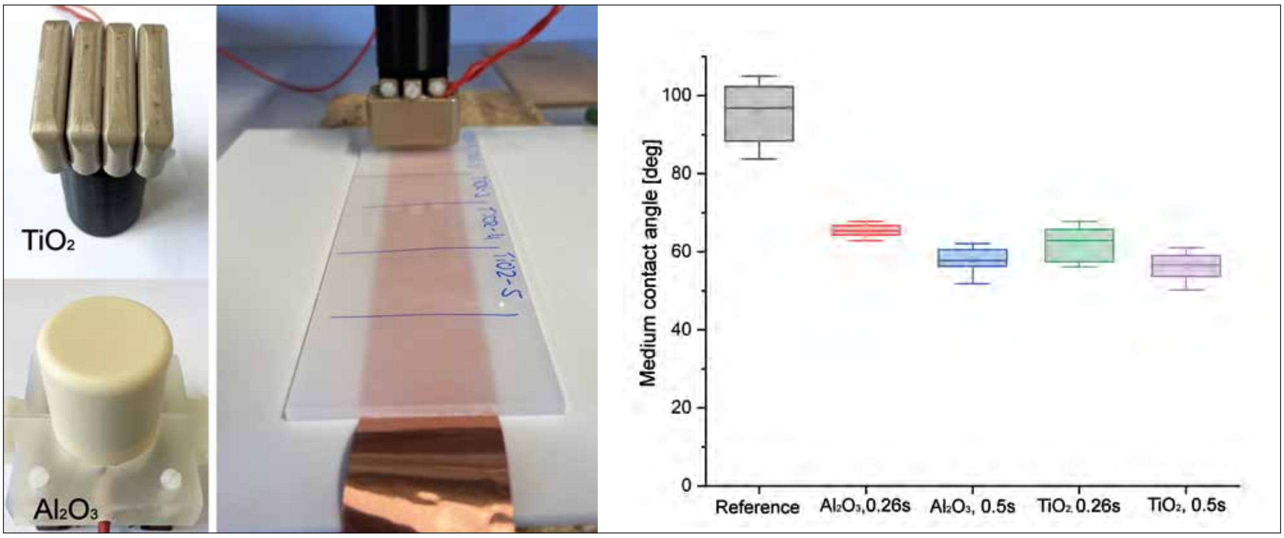

Fig. 13
Experimental set up for surface treatment of polypropylene (l.), and contact angle (r.)

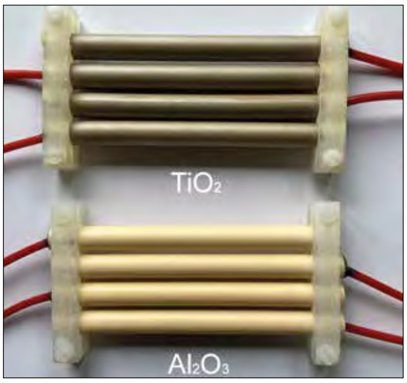

Fig. 14
Electrode configuration for ozone production with 120 mm long TiO_2 and Al_2O_3 tubes as dielectric

taining silver particles. For contacting, the surface was metallized with platinum and a wire was soldered by a standard leaded soft solder.

4 Electrodes in operation

The manufactured electrodes were characterised concerning long-term stability. Two electrodes were positioned parallel with a 3 mm gap (Fig. 11). A 50 Hz AC high voltage generator was used to generate a peak voltage of ±15 kV. At a power of 2,5–3 W a homogenous plasma was ignited and operated for 40 h. After different times of subjection to the plasma the weight was measured on a precision balance (±0,1 mg) and found to be constant. The surface roughness of the electrodes did not change as well over the operating time (Fig. 12). Since no significant loss of mass or change in roughness could be detected the titania electrodes show a good stability in the plasma. The treatment of materials with cold plasma to achieve certain surface properties is one of the main applications in industrial environments. For example, plastics or textiles can be cleaned and activated before subsequent coating. To validate the TiO_2/TiO_x electrodes, four TiO_2/TiO_x electrodes were stacked to form a total electrode with an edge length of 38 mm × 32 mm (Fig. 13).

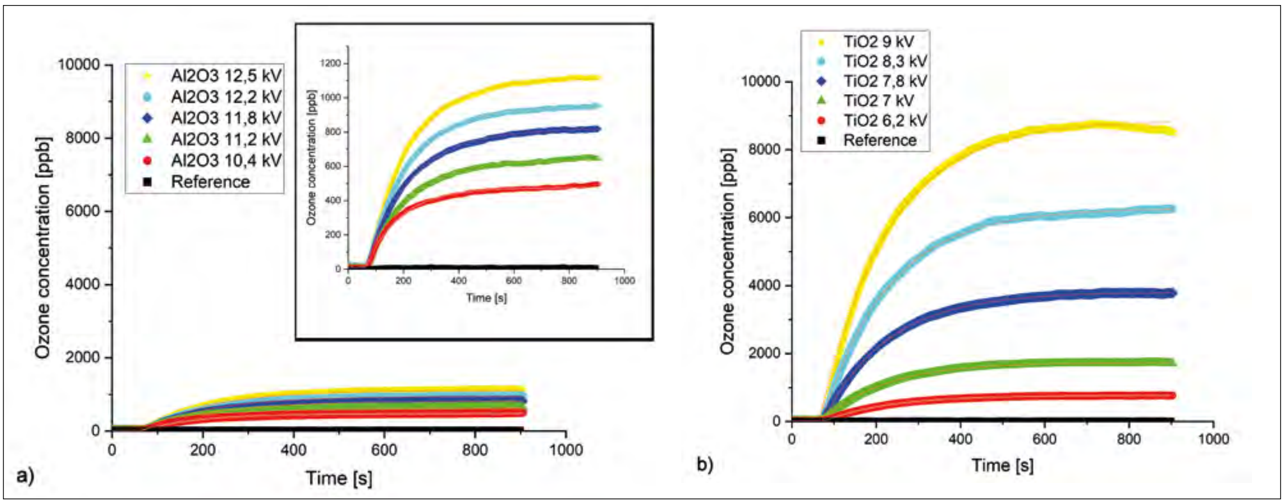

Fig. 15 a–b
Ozone concentration for a) Al_2O_3, and b) TiO_2 tubular electrodes at different voltages

This electrode stack was compared with an Al_2O_3 electrode, which was filled with bronze powder as the conducting part. The Al_2O_3 electrode had a cup shape with a diameter of 40 mm and 2 mm wall thickness. Both electrodes generated plasma to treat 3 mm thick Polypropylene (PP). The electrode distance to the polymer sheet was 3 mm. The PP had grounded copper tape on the opposite side. The high voltage generator produced a pulsed AC voltage of +21,3 kV and –22,4 kV at no load. Due to ignition, the voltage collapsed at a similar value (+19 kV and –18 kV) for the Al_2O_3 and the TiO_2/TiO_x electrode.
This is mainly due to the reason that the PP is the dominant dielectric in this setup. The pulse frequency was 247 kHz and the pulse repetition frequency was 10 kHz. After treatment, the activation of the substrate was characterised by measuring the contact angle of water (Krüss Mobile Surface Analyser). The initial contact angle, before treatment, was 95,8°. That means the surface was hydrophobic. After plasma treatment for 260 ms, the mean contact angle decreased to 65,5° for the Al_2O_3 electrode and 62° for the TiO_2/TiO_x electrode. After 500 ms, the contact angle was 58,0° with the Al_2O_3 electrode and 56,4° with the TiO_2/TiO_x electrode. Thus, surface

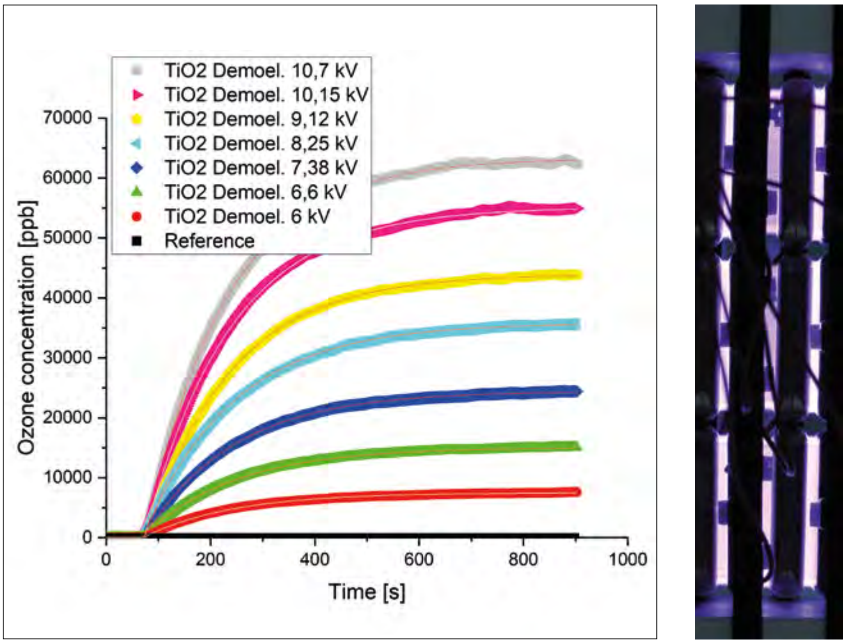

Fig. 16
Ozone concentration for 12 stacked titania electrodes (l.), and experimental setup in operation (r.)

tension towards water was decreased and activation was achieved with both electrodes.
Decontamination of air by plasma is one of the most promising applications today, especially in the light of the current challenges of the Corona pandemic. Bacteria, viruses, or molecules are physically destroyed by direct impact of ions and electrons.
Moreover, ozone is created in the atmospheric plasma. Ozone is known for its antibacterial and virucidal effects as it attacks the bonds between atoms.
Since this mechanism is highly effective, we measured the ozone creation rate by

plasma. In a 96 000 cm^3 chamber, the ozone concentration was measured over 15 min at various electrode configurations and voltages. The humidity was 45 % r.h. and the temperature 24,4 °C. For comparing the different dielectrics Al_2O_3 and TiO_2, the authors analysed geometrical identical tubes with 10 mm outer diameter, 6 mm inner diameter and 120 mm length. They were filled with bronze powder over a length of 100 mm, contacted, and externally cast with silicone. Four tubes were positioned with a spacing of 2 mm (Fig. 14). While voltages of 9 kV were sufficient for TiO_2 to obtain a uniform discharge pattern, 12,5 kV were required for Al_2O_3. Furthermore, despite the lower voltages, significantly higher ozone concentrations were achieved in the chamber. A higher voltage could not be applied to the TiO_2 electrodes due to the dielectric strength. While the Al_2O_3 only reached a concentration of 1100 ppb at 12,5 kV, the TiO_2 electrodes were already able to generate a concentration of 9000 ppb in the chamber at 9 kV (Fig. 15).

By using 12 electrodes described above, which were stacked three parts by four rows, the active area was increased to 63 m^2. They were operated under the same conditions as the tubes. At 9 kV 54 000 ppb ozone were created and at maximum voltage (10,7 kV) ozone concentration reached 63 000 bbp. Referring to the same applied voltage this is in the range of currently used equipment (Fig. 16).

5 Conclusions

Titania has been proven to be a suitable material for plasma electrodes. Its unique properties allow for long-term stable plasma electrodes. Especially the high permittivity enables the energy-efficient generation of plasma, as voltages can be reduced.

Their application for surface treatment of plastics and the formation of ozone has been shown.

Acknowledgments

The development work was performed within the IGF-project PlasmaEl (Grant No. 20546 BG). It was a project of the Research Association of the German Ceramic Society (FDKG) funded by the German Federation of Industrial Research Associations Otto von Guericke e.V. (AiF), within the framework of the program for the promotion of joint industrial research (IGF) funded by the Federal Ministry for Economic Affairs and Energy (BMWi).

The authors gratefully acknowledge the contributions of the companies of the Monitoring Committee (Aichinger, Coorstec, DBD Plasma, Dehn & Söhne, Edelstahl Nord, Phoenix Contact, Pro4Plasma, Venator). Thanks to Daniel Tasche and Rene Gropengießer from HAWK University of Applied Sciences and Arts for the great support and help. Thanks to the BMBF for funding the LSM 700 from Zeiss (Grant No.: 03FH008IN4).

References

[1] Pradeep, P.; Chulkyoon, M.: Non-thermal plasmas (NTPs) for inactivation of viruses in abiotic environment. Research J. of Biotechnology **11** (2016)

[2] Du, C.M.; Yan, J.H.: Surface sterilization by atmospheric pressure non-thermal plasma. In: Plasma remediation technology for environmental protection. Singapore 2017, 61–73

[3] Borchardt, T.; et al.: Effect of direct cold atmospheric plasma (di cap) on microcirculation of intact skin in a controlled mechanical environment. Microcirculation **24** (2017) [8]

[4] Helmke, A.; et al.: The acidification of lipid film surfaces by non-thermal DBD at atmospheric pressure in air. New J. of Physics. **11** (2009) 115025

[5] Gelker, M.; et al.: Influence of pulse characteristics and power density on stratum corneum permeabilization by dielectric barrier discharge. Biochimica et Biophysica Acta (BBA) – General Subjects **1863** (2019) [10] 1513–1523

[6] Gelker, M.; Müller-Goymann, C.; Viöl, W.: Plasma permeabilization of human excised full-thickness skin by µm and ns-pulsed DBD. Skin Pharmacology and Physiology. **33** (2020) [2] 69–76

[7] Mertens, N.; et al.: Inactivation of micro-organisms using cold atmospheric pressure plasma with different temporal discharge characteristics. Plasma Processes and Polymers **11** (2014) 910–920

[8] Xiao, G.; et al.: Non-thermal plasmas for VOCs abatement. Plasma Chemistry and Plasma Processing **34** (2014) 1033–1065

[9] ten Bosch, L.; et al.: Effects of newly devised plasma lice comb on human hair. Plasma Science and Technology **21** (2019) 125502

[10] ten Bosch, L.; et al.: Cold atmospheric pressure plasma comb – a physical approach for pediculosis treatment. Int. J. Environ. Res. Public Health **16** (2019) [1]

[11] Köhler, R.; et al.: Wood protection through plasma powder deposition – An alternative coating process Forests. Multidisciplinary Digital Publishing Institute. **10** (2019) 898

[12] Gascón-Garrido, P.; et al.: Copper and aluminium deposition by cold-plasma spray on wood surfaces: effects on natural weathering behaviour. Europ. J. of Wood and Wood Products **75** (2017) 315–324

[13] Zweynert, M.; et al.: Anwendung von Magnéli-Phasen des Titanoxids in der elektrochemischen Technologie. Chemie Ingenieur Technik **70** (1998) 827–841

[14] Eder, D.; Kramer, R.: Stoichiometry of titanium suboxide, Part 2 – Electric properties. Phys. Chem. 5, 1314–1319, DOI: 10.1039/b210004e (2003)

[15] Brevier Technische Keramik, Verband der Keramischen Industrie e.V., 2nd ed., Lauf 1998, 78,

[16] Moritz, T.: Ceramic injection moulding: Developments in production technology, materials, and applications. PIM Int. **14** (2020) [4]